

Modelling Concrete Soldier Pile Walls with Geometrical Non-Linearity of Vertical Piles

N. M. da C. Guerra¹, M. Matos Fernandes², A. S. Cardoso², A. Gomes Correia³

Summary

A significant part of urban excavations in Portugal is performed with anchored concrete soldier pile walls. Since large vertical loads are transmitted to the wall, design of the piles must include buckling and soil bearing capacity verifications. A simple method of updated coordinates for the consideration of buckling was implemented in a finite element code for the analysis of geotechnical works. The method is used in modelling an excavation supported by a concrete soldier pile wall. The importance of explicit consideration of geometrical non-linearities is emphasised.

Introduction

Excavations in urban area are frequently supported by anchored flexible retaining structures. In Portugal concrete soldier pile walls are often used. In this type of structure vertical soldier piles are installed in holes previously drilled in the ground on the perimeter of the excavation and a definitive concrete structure is then cast in place involving the piles. Figure 1 presents the construction procedure usually adopted.

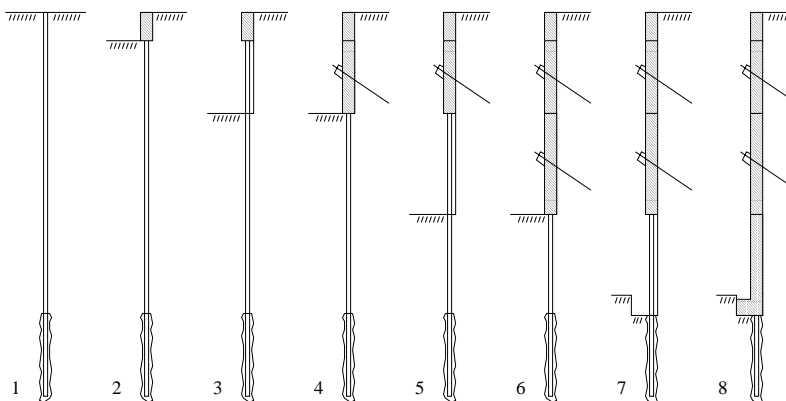


Figure 1: Construction process of concrete soldier pile walls.

Large values of vertical loads are usually applied to the piles, due to wall weight and anchor forces. Vertical equilibrium verification is, therefore, a relevant issue in the design of these walls. Instability can occur due to insufficient bearing capacity of the ground underneath the pile tip or by pile buckling. This last mode of failure is analysed in this paper, using the finite element method [1].

¹Instituto Superior Técnico, Lisbon, Portugal

²Faculty of Engineering, University of Oporto, Oporto, Portugal

³University of Minho, Guimarães, Portugal

Analysis of vertical instability by buckling is performed by explicitly considering the geometrical non-linearity, which is not usually available in finite element programs for geotechnical purposes. A simple method of updated node coordinates was implemented on a finite element code. In the first part of the paper this method is tested by comparison with theoretical solutions for simple cases and in the second part it is applied to the analysis of a supported excavation.

Tests of finite element program for determination of buckling loads

The problem presented in Figure 2 will be considered; the finite element mesh is represented in the same figure. The Euler critical load of the beam is

$$P_{cr} = \frac{\pi^2 EI}{L^2} = 73.5 \text{ kN/m} \quad (1)$$

where E is the young modulus, I is the moment of inertia of the beam section and L is the length of the beam. Axial load and bending moments are applied incrementally in such a way an eccentricity of $e = 0.115 \text{ m}$ is kept constant at all stages. A series of four calculation tests was undertaken, as described in Figure 2.

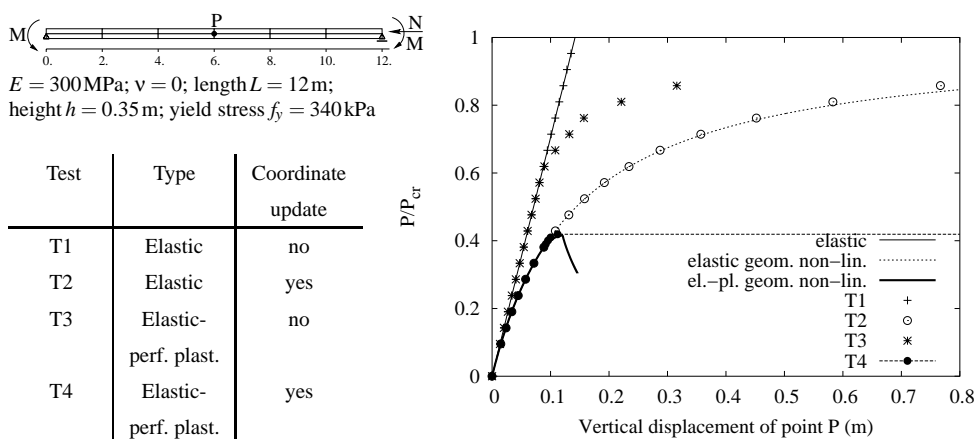


Figure 2: Tests T1 to T4 – main characteristics of the problem, finite element mesh and vertical displacement of point P versus axial load.

The figure also presents the axial load versus the vertical displacement of point P. For each test, the results are compared with the corresponding theoretical solutions. In both elastic and elastic-perfectly plastic cases with geometrical non-linearity the theoretical solutions were obtained assuming a parabolic deformation due to the moments applied at the extremities of the beam and a sinusoidal increase in displacement due to geometrical non-linearity. Some comments may be done:

- results from test T1 (elastic, no coordinate update) are naturally coincident with the theoretical solution;
- results from test T2 (elastic, with coordinate update) describes in a satisfactory way the theoretical behaviour up to an axial load of 80% of Euler critical load;

- results from test T3 are coincident with elastic results (T1) until plastification;
- results from test T4 (elastic-perfectly plastic, with coordinate update) are close to the theoretical solution; however, when the critical load is reached the iterative process no longer converges.

Eurocode 3 (EC3) [2] allows the determination of buckling load of steel elements (if no safety factors are used) and the calculation of an initial imperfection if geometrically non-linear effects are considered. A fifth test (T5) was carried out, using the example of a beam 3 m long with a section of a HEB120 of steel S235. HEB sections can not be exactly simulated using 2D finite elements; therefore, a similar section was simulated, using three rows of finite elements (flanges and web), corresponding to a “perfect” H, with square edges and no shape softening (see Figure 3).

Considering the flexural behaviour according to the axis of greater moment of inertia, because the thickness of the web is $t_w = 0.0065\text{ m}$ and the width of the flanges is $b = 0.12\text{ m}$, mechanical properties of the web are $t_w/b = 0.0065/0.12 = 0.054167$ times the mechanical properties of the flanges. Considering a Young modulus of 210 GPa and a yield stress of 235 MPa, the properties of the flanges will be the same ($E_f = 210\text{ GPa}$ and $f_{y,f} = 235\text{ MPa}$) and the properties of the web are $E_w = 11.375\text{ GPa}$ and $f_{y,w} = 12.729\text{ MPa}$.

Figure 3 also shows the results of buckling load and of the initial imperfection using EC3, as well as the finite element mesh used in the calculation test. The initial imperfections of sinusoidal and the maximum value is the one shown in the last column of the table (not perceptible in the finite element mesh). The graphic in Figure 3 shows the results of the test and it can be seen that the values obtained are close to the results from EC3.

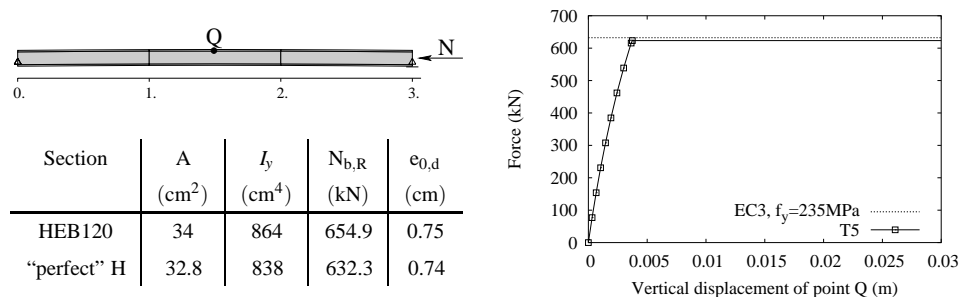


Figure 3: Test T5 – main characteristics of the problem, finite element mesh and vertical displacement of point Q versus axial load.

Numerical case study

Figure 4 presents the numerical case study analysed in this paper. The excavation is 20 m large and 18 m deep and is performed in clayey soil, supported by a concrete soldier pile wall, 0.4 m thick and with five anchor levels.

Horizontal components of anchor pre-stress are in equilibrium with the diagram also

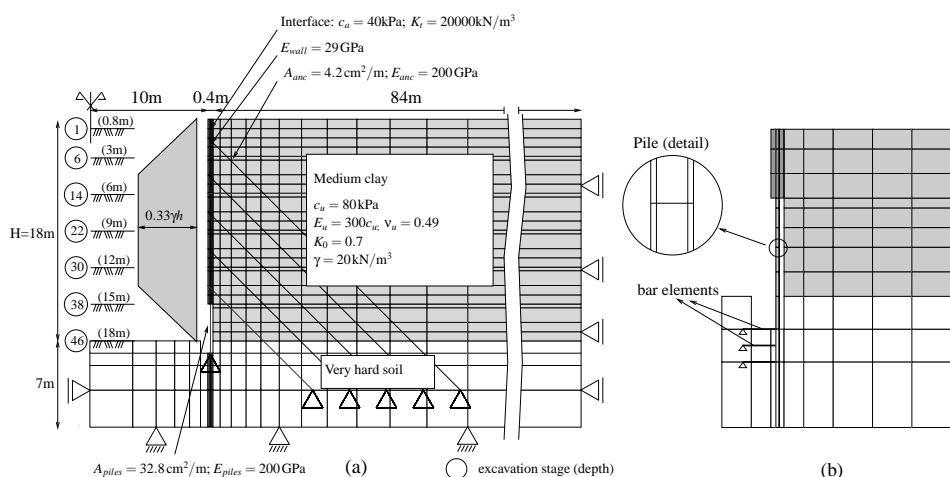


Figure 4: Geometry of the case study, material properties, finite element mesh at the last excavation stage (a) and detail of pile modelling (b).

represented in the figure; anchors are inclined at 45° with a pre-stress load of 458 kN/m. Vertical piles are HEB120 (S235) spaced 1 m. Soil and wall were modelled with isoparametric 8 noded finite elements; 6 noded joint elements were used to model the soil-to-wall interface; 2 noded bar elements were used to model anchors. Nodes in the seal zones of the anchors and of the piles are fixed points, located in the very hard ground below the excavated soil; it was assumed that they would not be affected by the excavation procedure.

Pile-wall interaction is considered through bar elements, also represented in Figure 4, assumed as elastic-perfectly plastic. The following reasons justify its use, instead of a direct contact between elements of the pile and elements of the soil: (a) the effect of soil-pile interaction is mainly 3D; its simulation in plane strain conditions would result in underestimating pile displacements; and (b) effects produced in the soil are very localized and globally less important than they would be if a direct contact between the pile and the soil would occur.

Both soil and soil-to-wall interface were analysed in total stress, with elastic-perfectly plastic behaviour, using Tresca yield criterium. Vertical piles were assumed elastic or elastic-perfectly plastic (depending on calculation).

Construction sequence is partially described in Figure 4; the indicated stages correspond to the end of each excavation level; excavation was performed removing one row of finite elements at each stage. Three analyses were performed – A, B and C, as described in Table 1.

In analyses A and B the entire excavation was simulated with convergence in every stage (tolerance of 0.1% for the residual forces). Analysis C was performed in an identical way until stage 29. At this stage, as illustrated by Figure 5, instability of vertical pile oc-

Table 1: Performed analyses

Analysis	Coordinate update	Pile resistance
A	no	unlimited
B	no	$f_{ym} = 249 \text{ MPa}$
C	yes	$f_{ym} = 249 \text{ MPa}$

curred by buckling and the iterative process diverged. The iterative process was therefore interrupted. It was considered that for maximum horizontal displacement of the pile greater than 1.0 m it was no longer possible to support any vertical loading. The elements representing the pile were, then, removed (Figure 5(c)) and the calculation could proceed (and converge) to stage 30, corresponding to the additional excavation of a row. In this analysis displacements reached, in stage 29 and, particularly, in stage 30, quite significant values.

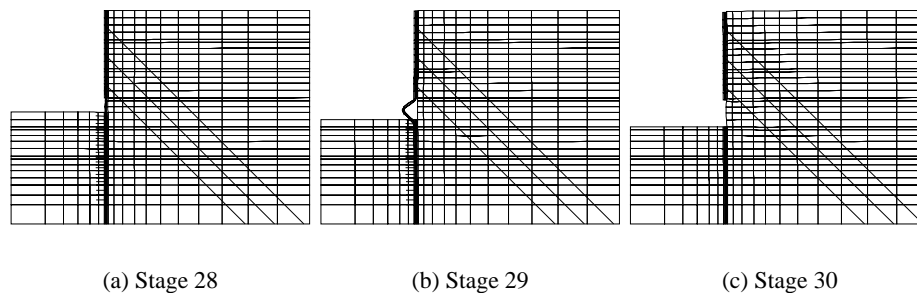


Figure 5: Deformed mesh of analysis C at stages 28, 29 and 30 (identical geometric and displacement scales).

Figure 6 shows the mobilised shear force at the soil-to-wall interface (a) and the mobilised resistance of the piles (b), assumed equal to $A_{pile}f_{ym}$ (mobilised resistance of the piles in analysis A is not presented because it was considered unlimited). In Figure 6(a) positive values of the shear force correspond to upward forces applied to the wall.

After an initial interface resistance mobilisation of analysis A, it can be observed a continuous decrease in this force; at the end of the excavation the interface shear force is applied downward to the wall in analysis A, which is the typical behaviour of flexible retaining structures with good foundation conditions.

Until stage 26 analyses A and B presented the same results; after this stage, there is an increase in the mobilised upward shear force for analysis B due to plastification of the piles and the consequent downward movement of the wall.

Analysis C provides almost the same results of analysis B until stage 27 (they are not exactly the same because this analysis is performed with updated coordinates). At stage 28 there is a substantial increase in the mobilised upward interface resistance. As it was observed, instability of the vertical pile occurs only in the next stage, where the iterative

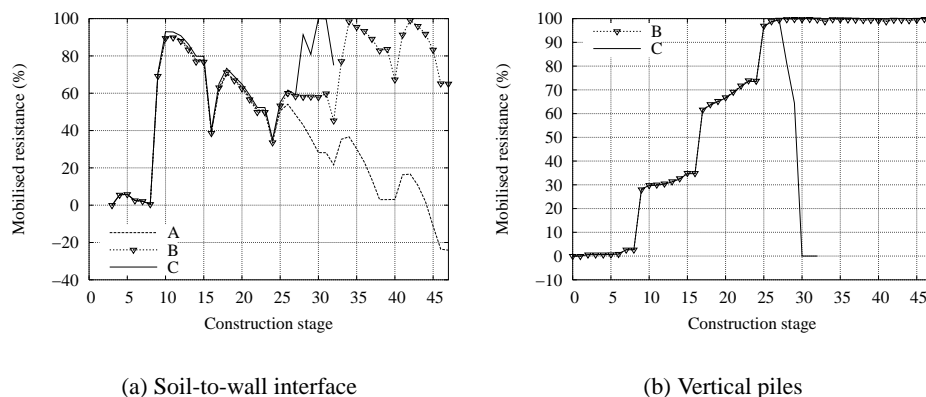


Figure 6: Mobilised resistance at the soil-to-wall interface and of the vertical piles for analyses A, B and C.

process did not converge, and therefore the calculated shear stresses must be observed with reserve. They are, however, quite large and would tend to the total interface resistance mobilisation, had the iterative process converged. It is however interesting to observe the forces at the vertical piles at stage 28 (see Table 2). At this stage there was an increase on the shear force, which means pile instability had already started.

Table 2: Forces on the vertical piles for analyses B and C (stages 27 to 30).

Stage:	27	28	29	30
Force: an. B (kN/m)	813	815	815	815
Force: an. C (kN/m)	813	663	526 (did not converge)	-

Conclusions

The simple procedure of coordinate update allows to model geometrical non-linearities which lead to buckling. This procedure was applied to a numerical case study of an excavation supported by a concrete soldier pile wall with poor vertical equilibrium conditions. The importance of explicit consideration of pile instability by buckling was shown and the process of loss of vertical equilibrium was analysed.

Reference

1. Guerra, N. M. da C. (1999): *Collapse mechanism of Berlin-type retaining walls by loss of vertical equilibrium*, Instituto Superior Técnico, Technical University of Lisbon, in Portuguese.
2. ENV 1993-1.1 (1992): *Eurocode3, Design of steel structures, Part 1.1, General rules and rules for buildings*, CEN, European Committee for Standardization.